NUCL SCI TECH (2016) 27:116
DOI 10.1007/s41365-016-0118-2

Rapid determination of radon monitor's calibration factors

Zhi-Qiang Li[1,2] · **De-Tao Xiao**[1] · **Gui-Zhi Zhao**[1] · **Xi-Jun Wu**[1] · **Jian Shan**[1] · **Qing-Zhi Zhou**[1] · **Zheng-Zhong He**[1]

Received: 9 February 2015 / Revised: 17 January 2016 / Accepted: 30 January 2016 / Published online: 29 August 2016

Abstract The monitors used to measure radon concentration must be calibrated, and the calibration factor of each measurement cycle should be determined. Thus, the determination time of calibration factors of NRL-II radon monitors should be reduced. In this study, a method is proposed to determine the calibration factors of radon monitors rapidly. In the proposed method, the calibration factor is initially determined in the 60-min measurement cycle; the calibration factor is then identified in the other measurement cycle on the basis of the principle that the calibration factor of the same radon monitor in different measurement cycles is inversely proportional to the number of α particles produced by ^{218}Po decay in this cycle. Results demonstrate that the calculated calibration factor of the different measurement cycles is consistent with the experimental calibration factor. Therefore, this method is reliable and can be used to determine the calibration factor of radon monitors rapidly.

Keywords Rapid determination · Radon concentration · Alpha particle number · Calibration factor

1 Introduction

Radon is a known carcinogen that can cause lung cancer. To control health risks, the World Health Organization proposed 100–300 Bq/m^3 as a reference range of radon in a residential area; beyond this range, an area is recommended for remediation [1]. As such, a continuous and reliable system of measurement should be developed to evaluate radon pollution in the environment [2, 3], to use radon as a tracer in various processes [4–7], such as earthquake prediction [8–10], and to conduct resource surveys [11, 12]. Radon concentrations in the environment are generally measured by sampling ambient air, passing the sample through a particulate air filter into a controlled chamber, and detecting the alpha particles emitted from short-lived decay products [13]. However, the recommended limit cannot indicate the changes in radon concentrations because the actual concentrations of this radioactive element in the environment vary greatly; thus, the currently applied methods cannot satisfy the requirement of a rapid and reliable measurement [14].

To detect changes in environmental radon concentration rapidly, researchers applied the electrostatic collection of ^{218}Po, which is the first-generation progeny of ^{222}Rn decay. The alpha particles produced from this decay are identified and counted; radon concentration is then calculated [15]. A NRL-II radon monitor developed by the University of South China is based on the principle of ^{218}Po collection by using an electric field in a semiconductor detector [16, 17]; the monitor is used to measure the radon concentration in air by using a cylindrical metal chamber to sample radon gas-containing environmental air actively. With this monitor, measurement cycles of 15 min, 30 min, and 60 min can be set to measure radon concentrations selectively.

The monitors used to measure the radon concentration must be calibrated; in radioactivity determination, statistical variation is high; as such, radon concentrations should be repeatedly determined to obtain an accurate calibration factor of each measurement cycle [18]. In this study, an

---

✉ De-Tao Xiao
13307478601@189.cn

Zhi-Qiang Li
hysylzq@126.com

[1] University of South China, Hengyang 421001, China

[2] Hengyang Normal University, Hengyang 421008, China

NRL-II radon monitor is developed on the basis of the principle that the calibration factor of the same radon monitor in different measurement cycles is inversely proportional to the number of α particles produced by ^{218}Po decay in this cycle to reduce measurement time; using this monitor, we initially determine the calibration factor in a 60-min measurement cycle and then calculate other degrees of radioactivity. Thus, statistical fluctuation can be reduced by extending the measurement time, and the calibration factor of the proposed radon monitor can be rapidly determined.

2 Methods and materials

2.1 Sampling circuit and collection cell

Figure 1 illustrates the collection cell of the NRL-II radon monitor and the detector assembly. The system comprises a cylindrical stainless steel vessel, a passivated implanted planar silicon (PIPS) detector, an amplifier circuit, a high-voltage divider, and a feedthrough. A positive high voltage is supplied to the *p* layer of the PIPS detector, and an electric field is produced in the vessel. The positively ionizing daughter nuclei are collected on the detector surface. The energy of α decay is then measured.

The stainless steel vessel exhibits the following dimensions: 11 cm in diameter, 10 cm in height, and 950 ml in volume. The inner portion of the vessel is electropolished to achieve a low background level. The PIPS detector is electrically isolated from the stainless steel vessel with an acrylic plate and a ceramic feedthrough. The following parameters are also set: detection area, 314 cm^2; sensitive thickness, 500 μm, and leakage current, 50 nA.

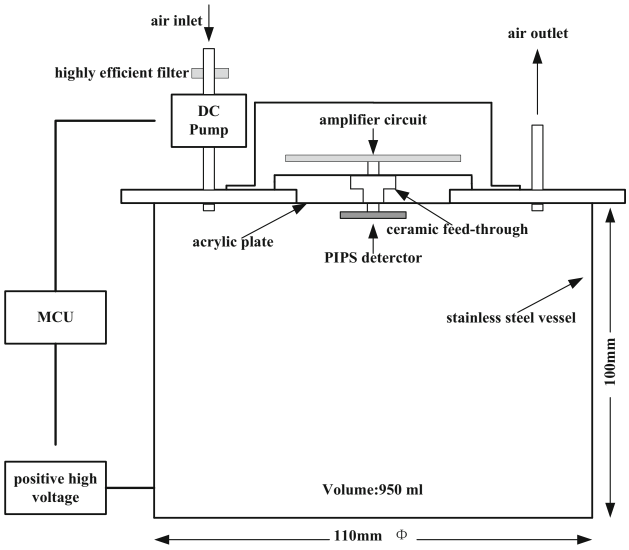

Fig. 1 Schematic of the collection cell of the NRL-II radon monitor

2.2 Principle of measurement

The NRL-II radon monitor was used to measure the radon concentrations. Air is initially sampled at a rate of 2.0 LPM by using a highly efficient filter paper head into the chamber with a DC pump-controlled MCU at the working T_s. The 3-kV positive high voltage (HV) is turned on. As ^{222}Rn decays, the positive charges of the first-generation progeny of ^{218}Po are absorbed on the semiconductor surface under the influence of an electrostatic field. As the progeny continuously decays, the energy of the α particles at the collection time T_{M} is determined using the semiconductor detector, and the radon concentration is calculated on the basis of the relationship between the number of α particles and the radon concentration (calibration factor). The ^{222}Rn concentration is calculated through electrostatic collection, as expressed in the following equation:

$$C_{^{222}\mathrm{Rn}} = K\eta VR\Delta N_{\mathrm{P}}(T), \tag{1}$$

where $C_{^{222}\mathrm{Rn}}$ is the radon concentration that should be measured in a specific environment, R is the correction factor of temperature and humidity [19], η is the detection efficiency, ΔN_{P} is the number of alpha particles after the first-generation progeny ^{218}Po further decays, K is the calibration factor of a radon monitor, and V is the volume of the chamber that should be measured. Equation (1) shows the detection efficiency.

The number of α particles collected by the detectors after ^{218}Po decays is expressed as follows:

$$\Delta N_{\mathrm{P}}(T_0)' = \eta VR\Delta N_{\mathrm{P}}(T_0). \tag{2}$$

Thus, Eq. (1) can be rewritten as follows:

$$C_{^{222}\mathrm{Rn}} = K\Delta N_{\mathrm{P}}(T)'. \tag{3}$$

If the decay constants and the intensity of ^{222}Rn radioactivity are λ_R and A_R, respectively, the corresponding decay constants and the intensity of ^{218}Po radioactivity are λ_P and A_P, respectively. At time t, the numbers of nuclei in ^{222}Rn and ^{218}Po atoms are $N_R(t)$ and $N_{\mathrm{P}}(t)$, respectively. Hence, $N_{\mathrm{P}}(t) = 0$ when $t = 0$, and

$$N_R(t) = N_R(0)\mathrm{e}^{-\lambda_R t}. \tag{4}$$

The radioactivity of ^{222}Rn is expressed as follows:

$$A_R(t) = \lambda_R N_R(t) = \lambda_R N_R(0)\mathrm{e}^{-\lambda_R t}. \tag{5}$$

The change in the number of nuclei in ^{218}Po atoms per unit time can be calculated from ^{222}Rn on the basis of the rate $\lambda_R N_R(t)$. However, ^{218}Po can decay into ^{214}Bi, which is expressed as $\frac{\mathrm{d}N_{\mathrm{P}}(t)}{\mathrm{d}t}$:

$$\frac{\mathrm{d}N_{\mathrm{P}}(t)}{\mathrm{d}t} = \lambda_R N_R(t) - \lambda_P N_{\mathrm{P}}(t). \tag{6}$$

Substituting Eqs. (6) with (5), we obtain the following expression:

$$N_{\mathrm{P}}(t) = \frac{\lambda_R}{\lambda_P - \lambda_R} N_R(0)(\mathrm{e}^{-\lambda_R t} - \mathrm{e}^{-\lambda_P t}). \tag{7}$$

According to Eq. (7), the activity of ^{218}Po can be expressed as follows:

$$A_P(t) = \lambda_P N_R(t) = \frac{\lambda_R \lambda_P}{\lambda_P - \lambda_R} N_R(0)(\mathrm{e}^{-\lambda_R t} - \mathrm{e}^{-\lambda_P t}). \tag{8}$$

We can then obtain Eq. (9) from the number of decayed ^{218}Po atoms from T_s to T on the basis of Eq. (8):

$$\Delta N_{\mathrm{P}}(T) = \int_0^{T_{\mathrm{M}}} \frac{\lambda_R \lambda_P}{\lambda_P - \lambda_R} N_R(0)(\mathrm{e}^{-\lambda_R t} - \mathrm{e}^{-\lambda_P t}). \tag{9}$$

To simplify Eq. (9), we derive the following equation:

$$\Delta N_P(T) = \frac{\lambda_R \lambda_P}{\lambda_P - \lambda_R} N_R(0) \left[\frac{1}{\lambda_R}\left(1 - \mathrm{e}^{-\lambda_R T_{\mathrm{M}}}\right) - \frac{1}{\lambda_P}\left(1 - \mathrm{e}^{-\lambda_P T_{\mathrm{M}}}\right) \right], \tag{10}$$

where T is the measurement cycle, which includes T_{S} and T_{M}, T_{S} is the sampling time, and T_{M} is the measurement time. If $T = 60$ min, the calibration factor of the measurement cycle ($T_{\mathrm{M}} = 3300$ s) is K_0. According to Eq. (3), (11) is obtained:

$$K_0 = \frac{C_{^{222}\mathrm{Rn}}}{\Delta N_{\mathrm{P}}(T_0)'}, \tag{11}$$

where K_x is the calibration factor of the other measurement cycles on the basis of Eqs. (1) and (9):

$$K_x = \frac{\Delta N_{\mathrm{P}}(T_0)}{\Delta N_{\mathrm{P}}(T_x)} K_0. \tag{12}$$

Equation (9) can be substituted into Eq. (12) to obtain Eq. (13):

$$K_x = \frac{\frac{1}{\lambda_R}\left(1 - \mathrm{e}^{-\lambda_R T_{\mathrm{M0}}}\right) - \frac{1}{\lambda_P}\left(1 - \mathrm{e}^{-\lambda_P T_{\mathrm{M0}}}\right)}{\frac{1}{\lambda_R}\left(1 - \mathrm{e}^{-\lambda_R T_{\mathrm{M}x}}\right) - \frac{1}{\lambda_P}\left(1 - \mathrm{e}^{-\lambda_P T_{\mathrm{M}x}}\right)} K_0. \tag{13}$$

Equation (13) shows that the calibration factor of the same radon monitor is associated with measurement cycle and sampling time, but not with collection and detection efficiency. The calibration factor of the radon monitor measured in any cycle at any sampling time can be calculated. The following equation can be used when the same radon monitor is used to experimentally obtain the calibration factor K_0, which is 60 min, to rapidly determine the radon concentration. To calculate the calibration factor in different measurement cycles, we set the following parameters: $T_s = 300$ s, $\lambda_R = 2.1 \times 10^{-6}\ \mathrm{s}^{-1}$, and $\lambda_P = 3.7 \times 10^{-3}\ \mathrm{s}^{-1}$; T_{M} is 600 and 1500 s when T and the measurement cycle are 15 and 30 min, respectively. The calibration factors K_{15} and K_{30} are expressed as follows:

$$K_{15} = 8.42 K_0, \tag{14}$$

$$K_{30} = 2.46 K_0. \tag{15}$$

Equations (13) and (14) show that a lengthy measurement cycle corresponds to a low calibration factor when the sampling time is fixed.

3 Experimental setup

Our calibration system (Fig. 2) is composed of the standard chamber, manifolds, PQ2000, and three improved NRL-II radon monitors. The calibration factor K is obtained as follows: The three radon monitors and PQ2000 are turned on for 1 h to allow these components to work synchronously. The background count of the radon monitors and air n_b is initially determined and the radon-containing air is removed. By this time, $\Delta N_{\mathrm{P}}(T)'$ or the gross count of ^{218}Po α particles radiates in the chamber. The mean value of the radon concentration $C_{^{222}\mathrm{Rn}}$ can then be obtained by PQ2000, and the value of the calibration factor K is obtained on the basis of Eq. (11). To maintain a stable $C_{^{222}\mathrm{Rn}}$ in the chamber, we use the standard radon chamber with a volume of 25 m^3 from the University of South China, and the steam leakage rate of the entire system is <0.10 %. The system is also equipped with an air-conditioning unit to regulate temperature and humidity with dynamic stability. The radon concentration of the chamber is set at 2500 Bq m^{-3} to reduce the influence of errors caused by radioactivity statistics. The stable temperature and humidity

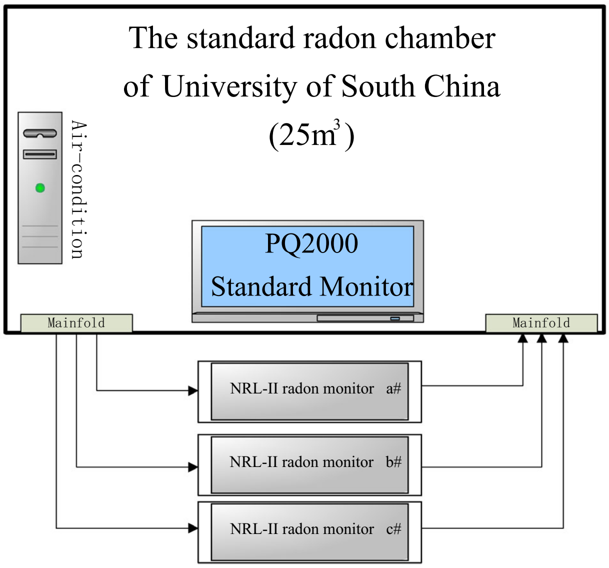

Fig. 2 NRL-II radon monitor calibration system

Table 1 Comparison between theoretical and experimental calibration factors of three NRL-II continuous radon monitors

T (min)	Number	Theoretical calibration factor ($\mathrm{Bq\,m^{-3}\,cpm^{-1}}$)	Experimental calibration factor ($\mathrm{Bq\,m^{-3}\,cpm^{-1}}$)				Errors (%)
			1	2	3	Average	
15	a	13.63	14.35	14.08	13.69	14.04	3.00
15	b	16.92	17.47	17.85	17.02	17.44	3.07
15	c	13.22	14.08	13.16	13.79	13.67	3.40
30	a	3.99	4.01	3.9	4.13	4.01	0.50
30	b	4.94	5.11	5.08	4.89	5.03	1.82
30	c	3.86	3.82	3.85	3.97	3.88	0.51
60*	a	–	1.64	1.60	1.61	1.62	–
60*	b	–	1.99	2.15	1.89	2.01	–
60*	c	–	1.58	1.60	1.53	1.57	–

* Cycles of 60 min of the experimental calibration factor as the standard calibration factor

are also maintained at 20 ± 2 °C and 45 ± 5 %, respectively. The detection efficiency η is different when the Ø20-mm detector of the *a* radon monitor is replaced with Ø30 mm. Moreover, the volume of the collecting cell is changed when the volume of the *b* radon monitor is adjusted from 950 to 785 ml.

4 Results and discussion

Three measurements are conducted using the three radon monitors with a cycle of 60 min (3600 s). The mean value of the radon concentration of the AlphaGUARD PQ2000Pro (Genitron Instruments GmbH, Germany) is considered the standard concentration of the chamber. Therefore, the average value of the three measurements and the calibration factor of each radon monitor with a cycle of 60 min can be obtained by using Eq. (13). The calibration factor can be obtained from the measurements of the three experiments: $K_{0a} = 1.62\ \mathrm{Bq\,m^{-3}\,cpm^{-1}}$, $K_{0b} = 2.01\ \mathrm{Bq\,m^{-3}\,cpm^{-1}}$, and $K_{0c} = 1.57\ \mathrm{Bq\,m^{-3}\,cpm^{-1}}$. K_{0a}, K_{0b}, and K_{0c} are substituted into Eqs. (14) and (15) to determine the theoretical values of K_{15} and K_{30}. The measurements are conducted thrice by using the three radon monitors with 15- and 30-min cycles. $C_{^{222}\mathrm{Rn}}$ is obtained again, and the mean value of the PQ2000Pro radon concentration is measured as the standard concentration of the chamber. The calibration factor K can be calculated according to Eq. (3). The calculated and measured data are listed in Table 1.

Table 1 shows that the experimental calibration factors of the radon monitor are consistent with the theoretical values, and the result is reliable. However, a large difference is observed when the three monitors are used at a measurement cycle of 15 min. Thus, the experimental calibration factors are significantly different from the theoretical calibration factors. Three reasons may contribute to this inaccuracy.

(1) Sufficient time is necessary to turn on high-voltage modules and reach a stable electric field. Using a high-voltage ammeter, we observe that 10 s is required to turn on our high-voltage modules. We then subtract 10 s from T_{M0} and $T_{\mathrm{M}x}$ and substitute the result in Eqs. (14) and (15) to obtain the following:

$$K_{15}^{*} = 8.60K_0, \tag{16}$$

$$K_{30}^{*} = 2.47K_0. \tag{17}$$

Thus, we can determine the relationship between the corrected determinations by substituting K_{0a}, K_{0b}, and K_{0c} of each monitor and the experimental calibration factor (Table 2). The corrected and experimental values are consistent with each other (Table 2). However, the *b* radon monitor exhibits greater inaccuracy than the *a* and *c* radon monitors after this correction is performed because the measurement cycle of the *b* radon monitor is relatively smaller than that of the two other monitors. As a

Table 2 Comparison between the revised theoretical and experimental calibration factors of the three NRL-II continuous radon monitors

T (min)	Number	Revised theoretical calibration factor ($\mathrm{Bq\ m^{-3}\,cpm^{-1}}$)	Average of experimental calibration factor ($\mathrm{Bq\,m^{-3}\,cpm^{-1}}$)	Errors (%)
15	a	13.63	14.04	0.79
15	b	17.28	17.44	0.92
15	c	13.50	13.67	1.25
30	a	4.00	4.01	0.25
30	b	4.97	5.03	1.20
3	c	3.88	3.88	0.00

consequence, a larger difference is observed. (2) In time-consuming measurements, the temperature and humidity of the collecting cell cannot be maintained at constant levels. Thus, a slight change can influence the efficiency of ^{218}Po collection and the results. (3) Radioactivity generally fluctuates.

Table 2 shows that the revised calibration factors of the different measurement cycles are consistent with the experimental calibration factors. Therefore, the proposed method can be used to determine the calibration factors of radon monitors rapidly and to improve the accuracy of continuous measurements.

5 Conclusions

In this study, a method is proposed to determine the calibration factors of radon monitors rapidly. We initially determine the calibration factor in the 60-min measurement cycle. The calibration factors in the other measurement cycles are then calculated on the basis of the principle that the calibration factor of the same radon monitor in a different measurement cycle is inversely proportional to the number of α particles produced by ^{218}Po decay in the same cycle. The experimental results demonstrate that the calculated calibration factor of the different measurement cycles is consistent with the experimental calibration factor. Therefore, this method can be used to determine the calibration factor of radon monitors rapidly.

Acknowledgments This study was supported by the National Natural Science Foundation of China (Grant Nos. 11475082, 11375083, and 11275096).

References

1. World Health Organization, *WHO handbook on indoor radon: a public health perspective* (World Health Organization, 2009). http://www.nrsb.org/pdf/WHO%20Radon%20Handbook.pdf
2. S.D. Chambers, F. Wang, A.G. Williams et al., Quantifying the influences of atmospheric stability on air pollution in Lanzhou, China, using a radon-based stability monitor. Atmos. Environ. **107**, 233–243 (2015). doi:10.1016/j.atmosenv.2015.02.016
3. F. Lamonaca, V. Nastro, A. Nastro et al., Monitoring of indoor radon pollution. Measurement **47**, 228–233 (2014). doi:10.1016/j.measurement.2013.08.058
4. D.E. Tchorz-Trzeciakiewicz, T. Parkitny, Radon as a tracer of daily, seasonal and spatial air movements in the Underground Tourist Route "Coal Mine"(SW Poland). J. Environ. Radioact. **149**, 90–98 (2015). doi:10.1016/j.jenvrad.2015.07.006
5. G. De Simone, G. Galli, C. Lucchetti et al., Using natural radon as a tracer of gasoline contamination. Procedia Earth Planet. Sci. **13**, 104–107 (2015). doi:10.1016/j.proeps.2015.07.025
6. T. Kuo, F. Tsunomori, Estimation of fracture porosity using radon as a tracer. J. Pet. Sci. Eng. **122**, 700–704 (2014). doi:10.1016/j.petrol.2014.09.012
7. C. Loisy, A. Cerepi, Radon-222 as a tracer of water–air dynamics in the unsaturated zone of a geological carbonate formation: example of an underground quarry (Oligocene Aquitain limestone, France). Chem. Geol. **296**, 39–49 (2012). doi:10.1016/j.chemgeo.2011.12.010
8. Q. Ye, R.P. Singh, A. He et al., Characteristic behavior of water radon associated with Wenchuan and Lushan earthquakes along Longmenshan fault. Radiat. Meas. **76**, 44–53 (2015). doi:10.1016/j.radmeas.2015.04.001
9. F. Külahcı, M. İnceöz, M. Doğru et al., Artificial neural network model for earthquake prediction with radon monitoring. Appl. Radiat. Isot. **67**(1), 212–219 (2009). doi:10.1016/j.apradiso.2008.08.003
10. E. Florido, F. Martínez-Álvarez, A. Morales-Esteban et al., Detecting precursory patterns to enhance earthquake prediction in Chile. Comput. Geosci. **76**, 112–120 (2015). doi:10.1016/j.cageo.2014.12.002
11. A. Pasculli, S. Palermi, A. Sarra et al., A modelling methodology for the analysis of radon potential based on environmental geology and geographically weighted regression. Environ. Model. Softw. **54**, 165–181 (2014). doi:10.1016/j.envsoft.2014.01.006
12. J. Elío, M.F. Ortega, B. Nisi et al., Evaluation of the applicability of four different radon measurement techniques for monitoring CO 2 storage sites. Int. J. Greenh. Gas Control **41**, 1–10 (2015). doi:10.1016/j.ijggc.2015.06.021
13. Y. Tan, D. Xiao, A novel algorithm for quick and continuous tracing the change of radon concentration in environment. Rev. Sci. Instrum. **82**(4), 043503 (2011). doi:10.1063/1.3572271
14. Y. Takeuchi, K. Okumura, T. Kajita et al., Development of high sensitivity radon detectors. Nucl. Instrum. Methods Phys. Res. A **421**(1), 334–341 (1999). doi:10.1016/S0168-9002(98)01204-2
15. A. Vargas, X. Ortega, J.L.M. Matarranz, Traceability of radon-222 activity concentration in the radon chamber at the technical university of Catalonia (Spain). Nucl. Instrum. Methods Phys. Res. A **526**(3), 501–509 (2004). doi:10.1016/j.nima.2004.02.022
16. L.I. Zhe, T.U.O. Xianguo, S.H.I. Rui et al., Analytic fitting and simulation methods for characteristic X-ray peaks from Si-PIN detector. Nucl. Sci. Tech. **24**(6), 060206 (2013). doi:10.13538/j.1001-8042/nst.2013.06.007
17. W. Fang-Fang, Z. Ze-Ran, Y. Yong-Liang et al., Calibration method for electrode gains in an axially symmetric stripline BPM. Nucl. Sci. Tech. (2014). doi:10.13538/j.1001-8042/nst.25.050102
18. A. Sorimachi, H. Takahashi, S. Tokonami, Influence of the presence of humidity, ambient aerosols and thoron on the detection responses of electret radon monitors. Radiat. Meas. **44**(1), 111–115 (2009). doi:10.1016/j.radmeas.2008.10.009
19. P. De Felice, X. Myteberi, The 222 Rn reference measurement system developed at ENEA. Nucl. Instrum. Methods Phys. Res. A **369**(2), 445–451 (1996). doi:10.1016/S0168-9002(96)80028-3